CHEMISTRY
A EUROPEAN JOURNAL

DOI: 10.1002/chem.200601287

Intramolecular Hydroamination/Cyclisation of Aminoallenes Mediated by a Neutral Zirconocene Catalyst: A Computational Mechanistic Study

Sven Tobisch*[a]

Abstract: The complete catalytic cycle for the intramolecular hydroamination/cyclisation (IHC) of 4,5-hexadien-1-ylamine (**1**) by a prototypical [$ZrCp_2Me_2$] precatalyst (**2**) has been scrutinized by employing a reliable DFT method. The present study conducted by means of a detailed computational characterisation of structural and energetic aspects of alternative pathways for all of the relevant elementary steps complements the mechanistic insights revealed from experimental results. The operative mechanism entails an initial transformation of precatalyst **2** into the thermodynamically prevalent, but dormant, bis(amido)–Zr compound in the presence of aminoallene **1**. This complex undergoes a reversible, rate-determining α-elimination of **1** to form the imidoallene–Zr complex. The substrate-free form, which contains a chelating imidoallene functionality, is the catalytically active species and is rapidly transformed into azazirconacyclobutane intermediates through a [2+2] cycloaddition reaction. This highly facile process does not proceed regioselectively because the alternative pathways for the formation of five- and six-membered azacycles have comparable probabilities. Degradation of cyclobutane intermediates by following the most feasible pathway occurs through protonolysis of the metallacycle moiety and subsequent proton transfer from the Zr–NHR moiety onto the azacycle. The five-membered allylamine is generated through protonation at carbon atom C^6 followed by α-hydrogen elimination, whereas protonolysis of the cyclobutane moiety at the Zr–N bond followed by proton transfer onto carbon atom C^5 is the dominant route for the six-membered product. Of the two consecutive proton transfer steps, the second one determines the overall kinetics of the entire protonation sequence. This process is predicted to be substantially slower than the cycloaddition reaction. The factors that regulate the composition of the cycloamine products have been elucidated.

Keywords: allenes · density functional calculations · hydroamination · reaction mechanisms · zirconium

Introduction

The catalytic, direct addition of amine R_2N–H bonds across a C–C multiple bond is of great interest both in academia and in industry. The intramolecular hydroamination/cyclisation (IHC) process represents the most efficient, concise and fully atom-economical means for the generation of functionalised azacycles from readily available and inexpensive starting materials. Functionalised nitrogen heterocycles are important for pharmaceuticals, for the synthesis of a variety of industrially relevant basic and fine chemicals, and as valuable chiral building blocks.[1] Cyclohydroamination can be mediated by early[2,3] and late[4] d-block transition metals, f-block elements[5,6] and also by calcium,[7a] gold[7b] and zinc[8] compounds, as reported recently. Organolanthanide and Group 4 metal compounds, in particular, are versatile and efficient catalysts for the IHC of various amine-tethered unsaturated carbon–carbon linkages. Titanium- and zirconium-based catalysts have provoked widespread interest,[9] owing to their general reactivity, ubiquitous availability and easy preparation, whereas the high sensitivity of organolanthanides[10] toward moisture and air limits their application.

Neutral[3a–e,h,i,11,12] and, more recently, cationic[3f,g,11b] titanium and zirconium compounds have been disclosed by several groups as effective catalysts for the IHC of various unsaturated C–C functionalities. A mechanism involving a catalytically active cationic metal–amido species, which is similar to that established for the organolanthanide-promoted process[6b,13,14] has been proposed for cationic Group 4 metal catalysts.[3g,15] In contrast, a metal–imido compound represents

[a] Dr. S. Tobisch
University of St Andrews, School of Chemistry
Purdie Building, North Haugh
St Andrews, Fife KY16 9ST (UK)
Fax: (+44) 1707-383-652
E-mail: st40@st-andrews.ac.uk

Supporting information for this article is available on the WWW under http://www.chemeurj.org/ or from the author.

the active catalyst species for neutral catalysts (see below) according to the mechanism firmly established for intermolecular hydroamination.[16–18]

Of the various unsaturated carbon–carbon linkages, aminoallenes are attractive substrates, for instance, owing to their potential for the tailored synthesis of N-heterocyclic skeletons that occur in biologically important compounds. Organolanthanides[19] and late transition-metal compounds[20] are known to catalyse aminoallene IHC. More recently, the groups of Bergman[11] and Johnson[12] have investigated the cyclohydroamination of aminoallenes promoted by neutral Group 4 metal compounds. Zirconocene precatalyst **2** has been reported to support the cyclisation of aminoallene substrate 4,5-hexadien-1-ylamine (**1**), albeit not regioselectively, to afford the six-membered imine as the predominant product (Scheme 1).[11b]

Herein, we present the first comprehensive computational exploration of the salient mechanistic features of aminoallene IHC supported by a neutral Group 4 metal compound, which has hitherto not been reported.[18] This study covers the complete IHC catalytic cycle and is aimed at complementing the mechanistic insights revealed from experiments by means of a detailed computational characterisation of structural and energetic aspects of alternative pathways for relevant elementary steps. These results will contribute to a deeper understanding of the factors that control the regioselectivity of the reaction.

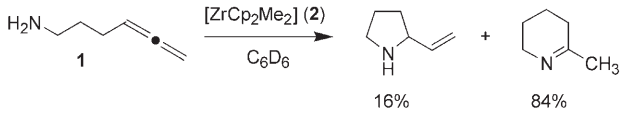

Scheme 1.

Catalytic Reaction Course

Neutral titanium and zirconium compounds have been reported to serve as effective precatalysts for the IHC of aminoallenes to afford functionalised five- and six-membered azacycles.[11] The original mechanism proposed by Bergman[16] for intermolecular hydroamination can also be adopted for cyclohydroamination. This mechanism has been confirmed by computational examination and through various experimental studies,[17] of which the detailed kinetic study by Doye[17a] is the most notable.[18] Scheme 2 shows a general catalytic cycle for neutral Group 4 metal-assisted cyclohydroamination of aminoallene substrate **1** by zirconocene complex **2**. Precatalyst **2** is transformed into the catalytically active imidoallene–Zr complex through protonolysis of the Zr–Me bonds by substrate **1**. The imidoallene–Zr

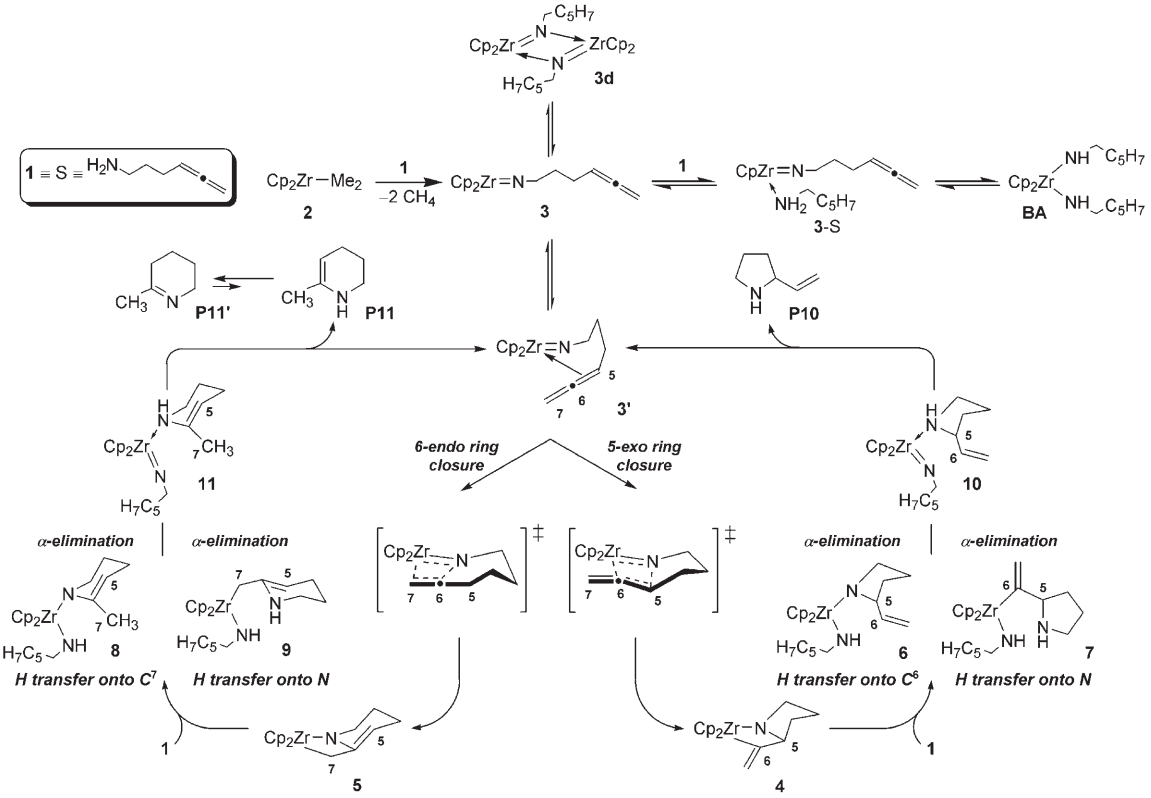

Scheme 2. General catalytic reaction course for the intramolecular hydroamination/cyclisation of aminoallenes to afford functionalised five- and six-membered azacycles, mediated by neutral Group 4 metal compounds, based on experimental studies by Bergman[16] and Doye.[17a] 4,5-Hexadien-1-ylamine (**1**) and [$ZrCp_2Me_2$] complex **2** were chosen as prototypical terminal aminoallene substrate and precatalyst, respectively.

complex can exist in substrate-free forms with a monohapto (**3**) or chelating (**3′**) imidoallene moiety, respectively, which can undergo dimerisation into **3d**. This compound can also complex additional **1** to form a stable substrate adduct (**3**-S), and can be converted into bis(amido)–Zr compound **BA** through α-abstraction of a proton. Subsequently, the allenic C=C linkage adds across the Zr=N bond through a [2+2] cycloaddition reaction. Ring closure can proceed through regioisomeric 5-*exo* and 6-*endo* pathways, thereby affording azazirconacyclobutane intermediates **4** and **5,** which contain five- and six-membered rings, respectively. Protonolytic cleavage of **4** and **5** by substrate **1** forms azacycle–amido–Zr compounds **6**–**9** through various reaction pathways. Subsequent α-hydrogen elimination yields cycloamine–imido–Zr complexes **10** and **11**, from which cycloamine products **P10** and **P11** are liberated to regenerate the catalytically active imidoallene–Zr complex and complete the cycle. Protonolytic cleavage of Zr–C^6 or Zr–N bonds in **4** followed by α-elimination yields 2-vinyl-pyrrolidine **P10**. Proton transfer onto the C^7 or N centre of **5** and subsequent α-elimination affords 6-methyl-1,2,3,4-tetrahydropyridine **P11** in both cases. Afterwards, product **P11** is likely to be readily transformed into thermodynamically favourable 2-methyl-3,4,5,6-tetrahydropyridine (**P11′**) through a 1,3-hydrogen shift.

Computational Model and Method

Model: In this DFT investigation, we report the exploration of the IHC of aminoallene substrate **1** by zirconocene precatalyst (**2**) as an archetypical neutral Group 4 metal compound. The studies encompass scrutinising alternative pathways for each of the elementary steps of the catalytic cycle displayed in Scheme 2.

Method: All DFT calculations were performed by using the program package TURBOMOLE[21] using the BP86 density functional[22] in conjunction with flexible basis sets of triple-ζ quality (see the Supporting Information for further details). The influence of the solvent (benzene)[11b] was taken into explicit consideration by making use of a continuum model. All the key species were fully located with inclusion of solvation by using the COSMO method.[23] The mechanistic conclusions drawn in this study were based on the computed Gibbs free-energy profile of the overall reaction. The suitability of the BP86 functional for the reliable determination of structural and energetic aspects of Group 4 metal-mediated cyclohydroamination has been demonstrated previously.[15] Further details of the computational methodology employed are given in the Supporting Information. All the drawings were prepared by employing the StrukEd program.[24]

Results and Discussion

Computational examination of the aminoallene IHC starts with a detailed step-by-step exploration of the elementary steps outlined in Scheme 2. To elucidate the selectivity control, various conceivable pathways for each of these steps have been scrutinised. The discussion will concentrate on the favourable pathway for a given step, whereas alternative, but less likely, pathways are referred to only briefly. The resulting free-energy profile of the overall process and the regulation of regioselectivity are discussed below.

Exploration of crucial elementary steps

Precatalyst activation: Effective catalysis entails the initial smooth transformation of precatalyst **2** into the imidoallene–Zr complex (Scheme 2). Alternative pathways for this conversion have been studied (Scheme 3). The energetics are collected in Table 1, whereas structural aspects of the key species can be found in Figure S1 in the Supporting Information.

Table 1. Enthalpies and free energies of activation and reaction for the conversion of precatalyst **2** into imidoallene–Zr and bis(amido)–Zr complexes.[a-c]

Conversion pathway	Substrate encounter complex	TS	Products[d]
1+**2**→**I1**+CH_4	6.1/*14.6* (**2**-S)	21.4/*30.5*	−25.1/*−23.0* (**I1**)
I1→**3′**+CH_4		31.6/*30.9*	18.5/*9.7* (**3**)
			9.9/*3.9* (**3′**)
I1+**1**→**BA**+CH_4	14.7/*22.3* (**I1**-S)	31.8/*40.3*	−18.6/*−17.2* (**BA**)
BA→**3**-S→**3′**+**1**		31.6/*31.3*	14.2/*13.8* (**3**-S)
			37.1/*26.9* (**3**)
			28.5/*21.1* (**3′**)

[a] See Schemes 2 and 3. [b] The activation barriers and reaction energies are given relative to the respective precursor species. [c] The enthalpies and free energies of activation ($\Delta H^{\neq}/\Delta G^{\neq}$) and reaction ($\Delta H/\Delta G$) are given in kcal mol^{-1}; the numbers in italic type are the Gibbs free energies. [d] See the text (or Schemes 6 and S1) for a description of **3**-S, **3** and **3′**.

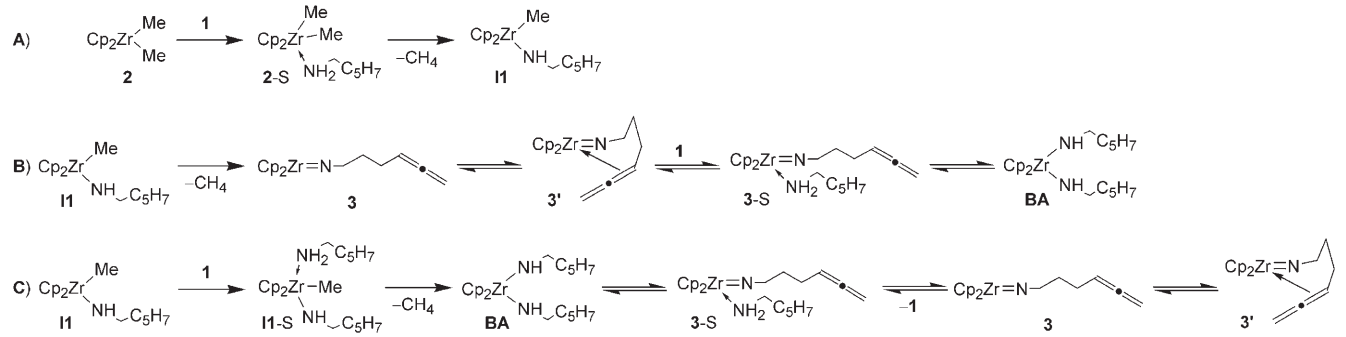

Scheme 3.

Firstly, one of the Zr–Me bonds of **2** is protonolytically cleaved by **1** to generate amidoallene-methyl–Zr intermediate **I1** with the liberation of methane (pathway A in Scheme 3). Subsequently, α-elimination of methane leads to the formation of the imidoallene–Zr complex, which can subsequently be transformed into bis(amido)–Zr compound **BA** through α-abstraction (pathway B in Scheme 3). Alternatively, the active catalyst complex can be formed through protonation of **I1** at the Zr–Me bond by an additional substrate molecule to give **BA**, followed by α-hydrogen elimination (pathway C in Scheme 3).

Protonolysis of the Zr–Me bond of **2** initially proceeds with the formation of substrate encounter complex **2**-S, which is uphill in enthalpy and free energy (Table 1).[25] Bond cleavage along pathway A (Scheme 3) requires a free energy of activation of 30.5 kcal mol^{-1} to form **I1** in an exergonic process with a reaction heat of −23.0 kcal mol^{-1} (Table 1). The **I1**→**3′**+CH_4 α-elimination step that follows (pathway B, Scheme 3) has a similar barrier of $\Delta G^{\ddagger}$ = 30.9 kcal mol^{-1} and the formation of **3′** is slightly endergonic (ΔG = 3.9 kcal mol^{-1}). Species **3′** readily complexes a substrate molecule to form adduct **3**-S (see below). The conversion of **3**-S→**BA** is kinetically feasible ($\Delta G^{\ddagger}$ = 17.5 kcal mol^{-1}) and driven by a thermodynamic force of −13.8 kcal mol^{-1} (Table 1). For the alternative **I1**+**1**→**BA**+CH_4→**3**-S route (pathway C, Scheme 3), the first protonolysis of the Zr–Me bond of **I1** is associated with a substantial barrier of $\Delta G^{\ddagger}$ = 40.3 kcal mol^{-1}, whereas the subsequent **BA**→**3**-S α-hydrogen elimination step is somewhat easier kinetically ($\Delta G^{\ddagger}$ = 31.3 kcal mol^{-1}, Table 1). Hence, **1**+**2**→**I1**(+CH_4)→**3**⇄**3′**(+2CH_4)+**1**⇄**3**-S⇄**BA** (pathways A and B, Scheme 3) is the favourable route for the conversion of precatalyst **2** into the imidoallene–Zr and bis(amido)–Zr complexes, respectively; this is consistent with experimental observations.[26] The route comprises of protonolytic Zr–Me bond cleavage (pathway A, Scheme 3), and α-elimination of methane (pathway B, Scheme 3), which have comparable kinetics ($\Delta G^{\ddagger}$ = 30.5–30.9 kcal mol^{-1}), followed by **3**-S⇄**BA** conversion ($\Delta G^{\ddagger}$ = 17.5 kcal mol^{-1}) through an α-abstraction pathway in the presence of additional substrate (Figure 1). The kinetics calculated for α-methane abstraction is in good agreement with the rate measured for 4-*tert*-butylaniline as a substrate,[27] thereby showing the suitability of the computational method employed for the reliable prediction of the energy profile.

Species **3′,** which contains a chelating imidoallene moiety, is prevalent among substrate-free forms **3** and **3′**, both of which are readily interconvertible (Scheme 6, Table 1 and Figure S1 in the Supporting Information).[25] Association of an additional substrate molecule to **3**⇄**3′** is kinetically facile[25] and thermodynamically favourable, which gives rise to **3**-S with an η^1-imidoallene moiety as the most stable adduct species (ΔG = −7.3 kcal mol^{-1} relative to {**3′**+**1**}, Table 1, Scheme 4). The imidoallene–Zr complex shows a propensity to form a dimer (**3d**).[26] The calculated thermodynamic force of −15.8 kcal mol^{-1} for **3′**⇄**3d** (Scheme 4) clearly shows that this equilibrium significantly favours **3d**.

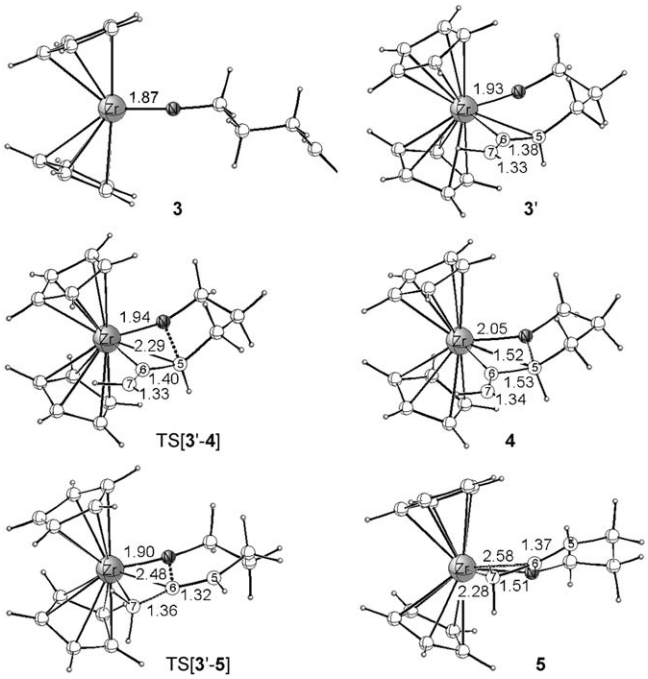

Figure 1. Selected structural parameters [Å] of the optimised structures of key species for 5-*exo* (top and middle) and 6-*endo* (bottom) ring closure. The cutoff for drawing Zr–C bonds was arbitrarily set to 2.8 Å. Please note that the imidoallene moiety is displayed in a truncated fashion for several of the species.

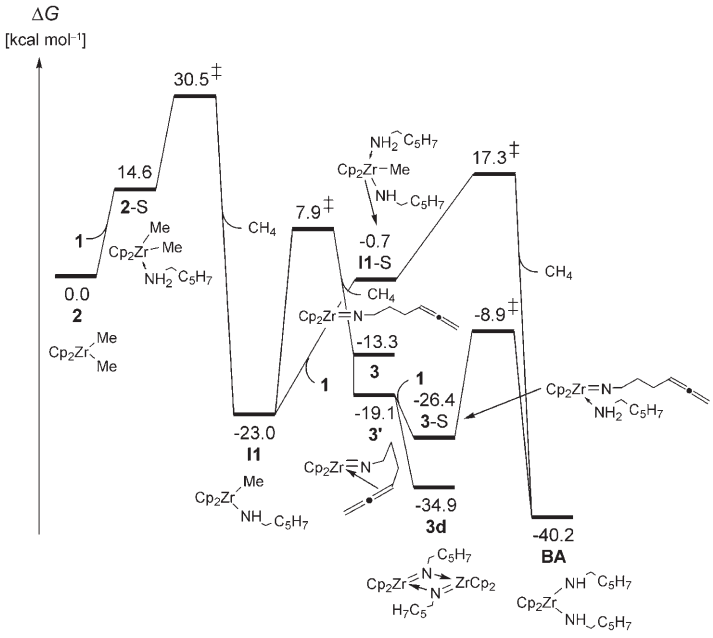

Scheme 4. Condensed Gibbs free-energy profile [kcal mol^{-1}] of the conversion of precatalyst **2** into the imidoallene–Zr and bis(amido)–Zr complexes.

The alternative **3′**+**1**⇄**3**-S⇄**BA** conversion is kinetically accessible ($\Delta G^{\ddagger}$ = 17.5 kcal mol^{-1}) and downhill by −21.1 kcal mol^{-1} (Table 1, Scheme 4).

Overall, the free-energy profile shown in Scheme 4 reveals that the imidoallene–Zr catalyst complex is predominantly present as dimer **3d** and is readily transformed into bis(amido)–Zr compound **BA**, which is most stable.[28] Complex **BA**[29] is a dormant species, which therefore necessitates conversion into **3** or **3′** to enter the productive catalytic cycle.[16,17a] However, this process has a free energy of activation of 31.3 kcal mol^{-1} and is thermodynamically disfavoured.

Intramolecular cycloaddition: The **3**⇄**3′** and **3**-S forms of the imidoallene–Zr complex can be equally envisaged as being the precursor for the [2+2] cycloaddition reaction of the allenic C=C linkage across the Zr=N bond. Alternative pathways, with or without additional substrate participation, have been scrutinised to identify the substrate-free species that participate along the minimum energy pathway for C–N bond formation (see below). The regioisomeric 5-*exo* and 6-*endo* pathways are structurally characterised in Figure 1, whereas the energy profiles are collected in Table 2.

Table 2. Enthalpies and free energies of activation and reaction for cycloaddition through regioisomeric 5-*exo* and 6-*endo* pathways.[a-c]

Ring closure	Precursor[d]	TS	Product[e]
5-*exo*	8.6/*5.8* (**3**)		
	0.0/*0.0* (**3′**)	0.5/*2.0*	−14.9/*−14.0* (**4**)
6-*endo*	8.6/*5.8* (**3**)		
	0.0/*0.0* (**3′**)	1.5/*2.3*	−29.3/*−27.8* (**5**)
	aminoallene substrate-assisted process[f]		
5-*exo*	−14.3/*−7.3* (**3**-S)		
	−10.6/*−3.4* (**3′**-S)	7.1/*15.6*	−15.0/*−5.4* (**4**-S)
6-*endo*	−14.3/*−7.3* (**3**-S)		
	−10.6/*−3.4* (**3′**-S)	8.7/*16.9*	−32.7/*−22.6* (**5**-S)

[a] See Scheme 2. [b] The activation barriers and reaction energies are given relative to the thermodynamically favourable isomer **3′**, which contains a chelating allene functionality. [c] The enthalpies and free energies of activation ($\Delta H^{\neq}/\Delta G^{\neq}$) and reaction ($\Delta H/\Delta G$) are given in kcal mol^{-1}; the numbers in italic type are the Gibbs free energies. [d] See the text (or Scheme 6) for a description of isomers **3** and **3′**. [e] See Scheme 2 for a description of the azazirconacyclobutane intermediates. [f] The process to be assisted by an additionally coordinating aminoallene molecule has been investigated for **1** as the substrate. The activation barriers and reaction energies are given relative to {**3′**+**1**}.

The prevalent species (**3′**) of the substrate-free forms with a chelating imidoallene moiety represents the direct precursor for both the 5-*exo* and 6-*endo* pathways. Following the two pathways, transition states are encountered that show a marginally distorted structure (Figure 1). These precursor-like transition state (TS) structures are indicative of a highly facile transformation. Indeed, cycloaddition reactions of **3′**→**4** and **3′**→**5** have comparable barriers that amount to only 2.0 and 2.3 kcal mol^{-1} ($\Delta G^{\neq}$, Table 2), respectively, and are exergonic. Of the two almost kinetically equivalent pathways, the 6-*endo* pathway is driven by a larger thermodynamic force of 27.8 kcal mol^{-1}.

As previously mentioned, the role of extra substrate molecules for intramolecular C–N bond formation has been explored explicitly (Figure S2 in the Supporting Information). Although **3′** readily complexes **1** to form a stable adduct (**3**-S), neither **4** nor **5** are stabilised in free energy upon uptake of **1** (Table 2). Unsurprisingly, transition states TS [**3′**-**4**] and TS [**3′**-**5**], which are already highly favourable, do not benefit from substrate association in terms of both enthalpy and free energy. Hence, excess substrate does not accelerate the cycloaddition reaction. As a consequence, the substrate must first dissociate from adduct **3**-S prior to ring closure through the **BA**⇄**3**-S⇄**3′**(+**1**)→**4**(+**1**) and **BA**⇄**3**-S⇄**3′**(+**1**)→**5**(+**1**) pathways, respectively.

Protonation of azazirconacyclobutane intermediates: Protonation of the azazirconacyclobutane intermediates in a stepwise fashion is encountered next in the course of the reaction (Scheme 2). Various conceivable pathways that commence from **4** and **5** have been critically explored. This section focuses primarily on the favourable pathways that are likely to be traversed in the catalytic cycle. They are characterised structurally in Figures 2 and 3 for the ones that commence from **4** and **5**, respectively, and the energetics are collected in Table 3. The full account of structural (Figure S3–9) and energetic aspects (Table S1) of all investigated pathways is included in the Supporting Information.

*Intermediate **4***: Cleavage of **4** by **1** can proceed along different pathways for protonation at the Zr–C^6 and Zr–N bonds of the metallacycle, thereby giving rise to azacycle–amido–Zr compounds **6** and **7**, respectively. Subsequent α-elimination leads to the formation of cycloamine-imido–Zr complex **10** in both cases, from which 2-vinylpyrrolidine (**P10**) is eventually released through the regeneration of the active imidoallene–Zr complex (Scheme 2).

Starting with protonolytic cleavage of the metallacycle, the first substrate association causes a relaxation of the ligand sphere around the Zr centre, but the metallacycle is still intact in **4**-S (Figure 2 and Figure S3 in the Supporting Information, top). Uptake of the substrate is kinetically facile[25] and to some extent downhill at the ΔH surface, however, this is not large enough to compensate for the associated entropy penalty (Table 3). Thus, **4**-S is uphill in free energy relative to {**4**+**1**}. Proton transfer onto the alternative C^6 or N centres of the metallacycle fragment evolves through a TS structure that constitutes concurrent amine N–H bond cleavage and C–H or azacycle N–H bond formation in the proximity of the Zr centre and leads to the formation of **6** and **7**, respectively.

Protonation at the Zr–C^6 bond along the **4**+**1**→**6** pathway is downhill with an exergonicity of −15.6 kcal mol^{-1} and is associated with a barrier that amounts to 18.3 kcal mol^{-1} (ΔG, $\Delta G^{\neq}$ relative to {**4**+**1**}, Table 3). The alternative **4**+**1**→**7** pathway has a lower barrier ($\Delta G^{\neq}$ = 14.3 kcal mol^{-1}) and is almost thermoneutral.

The TS structure for proton transfer onto the α-position of the azacycle moiety in **6** and **7** shows structural character-

Table 3. Enthalpies and free energies of activation and reaction for protonolytic cleavage of azazirconacyclobutane intermediates **4** and **5** by aminoallene **1** to afford cycloamine-imido–Zr compounds **10**, **11**, **11′** and **12** through various pathways for proton transfer.[a-c]

Proton transfer pathway	**4**/**5**-S[d]	TS	Product[d]
5-*exo* (**4**)			
H transfer onto C^6 of **4**	−0.1/*8.6* (**4**-S)	9.1/18.3	−24.0/*−15.6* (**6**)
6→**10**		29.0/*28.6*	14.2/*13.4* (**10**)
H transfer onto N of **4**	−4.6/*4.3* (**4**-S)	4.6/*14.3*	−8.2/*0.7* (**7**)
7→**10**		30.6/*30.1*	14.2/*12.6* (**10**)
6-*endo* (**5**)			
H transfer onto C^7 of **5**	−3.4/5.2 (**5**-S)	8.9/*17.9*	−23.9/*−15.7* (**8**)
8→**11**		32.4/*33.0*	19.8/*19.2* (**11**)
8→**11′**		40.5/*42.2*	8.4/*7.7* (**11′**)
H transfer onto N of **5**	−5.2/3.7 (**5**-S)	9.1/*18.2*	−13.5/*−4.8* (**9**)
9→**11**		34.8/*34.1*	9.4/*8.3* (**11**)
9→**12**		26.0/*26.3*	9.8/*8.1* (**12**)
		aminoallene substrate-assisted	
5-*exo* (**4**)			
4→**6**[f]		14.6/*31.3*	
6→**10**[f]		19.2/*26.9*	
4→**7**[f]		1.6/*18.8*	
7→**10**[f]		32.4/*39.3*	
6-*endo* (**5**)			
5→**8**[f]		15.7/*32.8*	
8→**11**[f]		22.0/*30.4*	
8→**11′**[f]		26.2/*34.2*	
5→**9**[f]		6.9/*24.1*	
9→**11**[f]		36.0/*42.9*	
9→**12**[f]		17.3/*24.8*	

[a] See Schemes 2 and 5. [b] The activation barriers and reaction energies are given relative to the respective precursor species. [c] Enthalpies and free energies of activation ($\Delta H^{\neq}/\Delta G^{\neq}$) and reaction ($\Delta H/\Delta G$) are given in kcal mol^{-1}; the numbers in italic type are the Gibbs free energies. [d] See the text (or Figures 2, 3 and S3–S5) for a description of the various isomers of amine adducts **4**-S and **5**-S and of cycloamine-imido–Zr product species **10**, **11**, **11′** and **12**. [e] The process to be assisted by an additional aminoallene molecule has been investigated with methylamine ($MeNH_2$, S′) as the substrate. The activation barriers are given relative to {precursor species + $MeNH_2$}. [f] The aminoallene acts as a mediating proton shuttle (Figures S7 and S9).

istics similar to those for the previous step (Figure 2 and Figure S3 in the Supporting Information, bottom). However, H-abstraction from the amidoallene moiety is calculated to be significantly less facile and requires a barrier of $\Delta G^{\neq}=28.6$–30.1 kcal mol^{-1} (Table 3) to be overcome. Hence, the second of the two consecutive protonation steps determines the overall kinetics for the conversion of **4**→**10**. As revealed from Table 3, the **4**+**1**→**6**→**10** pathway, which has the largest overall barrier of 28.6 kcal mol^{-1} (**6**→**10**) is predicted to be favourable. It is driven by a total thermodynamic force of −2.2 kcal mol^{-1} (relative to {**4**+**1**}). Subsequent cycloamine product release through the **10**→**P10**+**3′** pathway is kinetically facile[25] and slightly endergonic ($\Delta G=$ 1.6 kcal mol^{-1}).

A possible supportive role of excess substrate has been explicitly probed by using an additional methylamine molecule as model substrate S′. Two different scenarios have been investigated and characterised in previous computational studies.[14b,c,15,30] Firstly, additive S′ acts as a mediating agent for both of the consecutive proton transfer steps (Table 3, Figure 2, Figure S7 in the Supporting Information). Alternatively, an additionally coordinated substrate molecule serves as the proton source for the second protonation step (through **6**→**10** and **7**→**10**), which leads to the formation of a bis(amido)–Zr compound upon cycloamine release (Figure S6 in the Supporting Information). Complete characterisation of all the pathways that have been investigated is provided in the Supporting Information (Table S1, Figures S6 and S7). For a coordinated S′ molecule in the second protonation step, the located transition states TS[**6**–**10**]-S′ and TS[**7**–**10**]-S′ (Figure S6 in the Supporting Information) are lower in enthalpy than {TS[**6**–**10**]+S′} and {TS[**6**–**10**]+S′}, respectively. However, enthalpic stabilisation cannot counterbalance the entropy costs, so that excess substrate which serves as the proton source is not likely to facilitate the second protonation step. For the alternative scenario, in which proton transfer occurs through a TS structure with an external substrate moiety bearing a formally quaternary nitrogen centre (Figure S7 in the Supporting Information), protonation at the Zr–C^6 bond (via TS[**4**-**6**-S′] and TS[**7**-**10**-S′]) is disfavoured at the ΔH surface, whereas proton transfer onto the nitrogen centre of the azacycle (via TS[**6**-**10**-S′] and TS[**4**-**7**-S′]) is promoted. Notably, the second proton transfer step through TS[**6**-**10**-S′] benefits to a greater extent from an external substrate molecule than the first transfer step, but the overall kinetics is still dictated by the second protonation event. As a result, TS[**6**-**10**-S′] has a free energy that is lower than {TS[**6**-**10**]+S′} (Table 3). Hence, additional amine that can act as a "proton shuttle" appears to accelerate the **6**→**10** pathway.

Overall, **4**+**1**→**6**→**10** pathway is predicted to be the dominant route for the formation of vinylamines that leads to **P10** with an overall barrier of $\Delta G^{\neq}=26.9$ kcal mol^{-1} for the second substrate-assisted step.

Intermediate ***5***: Cleavage of the metallacycle of **5** by **1** through protonation at the Zr–C^7 and Zr–N bonds gives rise to **8** and **9**, respectively. These compounds can then undergo proton transfer onto the α-position of the coordinated azacycle to be transformed into **11** in both cases (Scheme 2). Alternatively, protonation can occur at the C^5 centre of **8** and **9**, thereby affording 2-methyl-3,4,5,6-tetrahydropyridine (**P11′**) and 2-methylenepiperidine (**P12**), respectively (Scheme 5). These two pathways require some initial rotations, which are kinetically easy, of the azacycle in **8** and **9** to align the C^5 centre *syn* to the amidoallene moiety.[31]

The various pathways investigated display structural features (Figure 3 and Figures S4 and S5 in the Supporting Information) that are similar to the protonation of **4**, which was analysed above. Substrate complexation onto **5** is facile[25] and endergonic (Table 3), which readily gives rise to precursor adduct **5**-S as a transient species. Similar to the findings for **4**, the first protonation step is predicted to be kinetically feasible and requires overcoming free-energy barriers of comparable magnitude (17.9–18.2 kcal mol^{-1} for **5**+**1**→**8**/**9**). Of the almost kinetically equivalent pathways, the **5**+**1**→**8** pathway is thermodynamically preferred (Table 3). The second protonation to follow the various pathways

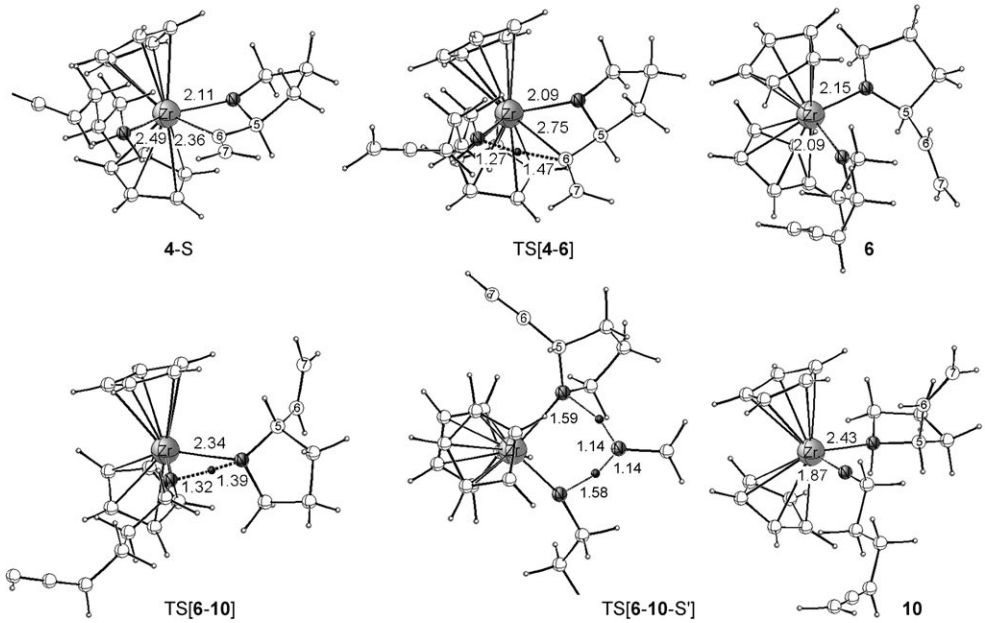

Figure 2. Selected structural parameters [Å] of the optimised structures of key species for protonolytic cleavage of the metallacycle in **4** by **1** to afford azacycle–amido–Zr compound **6** (top) and subsequent α-hydrogen abstraction to form cycloamine–imido–Zr complex **10** (bottom). See also Figures S6 and S7 in the Supporting Information. The cutoff for drawing Zr–C bonds was arbitrarily set to 2.8 Å. Please note that the amido-/imidoallene moiety is displayed in a truncated fashion for several of the species.

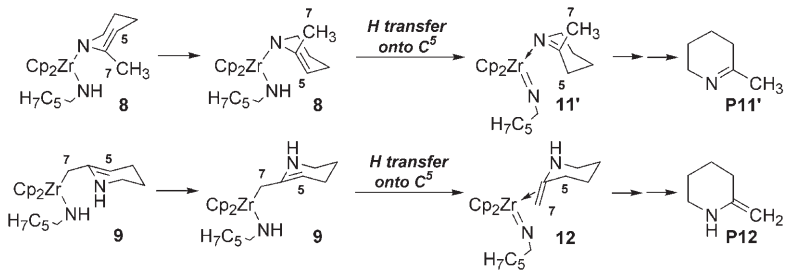

Scheme 5.

(Schemes 2 and 4) is associated with a significantly higher barrier that exceeds $\Delta G^{\neq} = 33$ kcal mol^{-1} in all but one case; this parallels the general features of the stepwise protonation discussed above for **4**. A notable exception is the proton transfer onto the C^5 centre of **9** to form **12** (Figure 3, bottom). This pathway has the lowest barrier ($\Delta G^{\neq} =$ 26.3 kcal mol^{-1}) of all the pathways investigated for the second protonation step, however, it is still kinetically more difficult than the first proton transfer. Hence, the second of the two consecutive protonation steps controls the overall kinetics. Consequently, the **5+1→9→12→3′+P12** pathway is predicted to be the most easily accessible of all the alternative protonation pathways that commence from **5**. This pathway leads to the formation of **P12** as the initial six-membered cycloamine in a process that is slightly endergonic overall ($\Delta G = 2.9$ kcal mol^{-1},[32] relative to {**5+1**}, Table 3). A subsequent 1,3-hydrogen shift converts **P12** into the more stable product **P11′** ($\Delta G = -6.5$ kcal mol^{-1}).[33]

With regards to the supportive influence of additive substrate (the full account of all pathways studied is included in Table S1, Figures S8 and S9 in the Supporting Information), a similar picture to that discussed above for **4** is revealed. Therefore, the focus here is on the second protonation step, for which molecule S′ acts as a proton shuttle, namely, to transfer a proton onto the nitrogen centre of the azacycle (**8→11**), and also to transfer a proton onto carbon atom C^5 of the azacycle (**8→11′** and **9→12**; Figure S9 in the Supporting Information). For all these pathways, the external substrate stabilises the transition state at the ΔG surface (Table 3), which indicates that these pathways are accelerated by using excess substrate. Similar to the findings for the protonation of **4**, additive substrate does not change the relative kinetics of different pathways. Firstly, the second of the two consecutive proton transfer steps dictates the overall kinetics, and secondly, the **5+1→9→12→3′+P12** pathway, which has an overall barrier of $\Delta G^{\neq} = 24.8$ kcal mol^{-1} for the **9→**TS[**9-12**-S′]**→12** substrate-assisted step, is kinetically the most feasible pathway of all the competing routes.

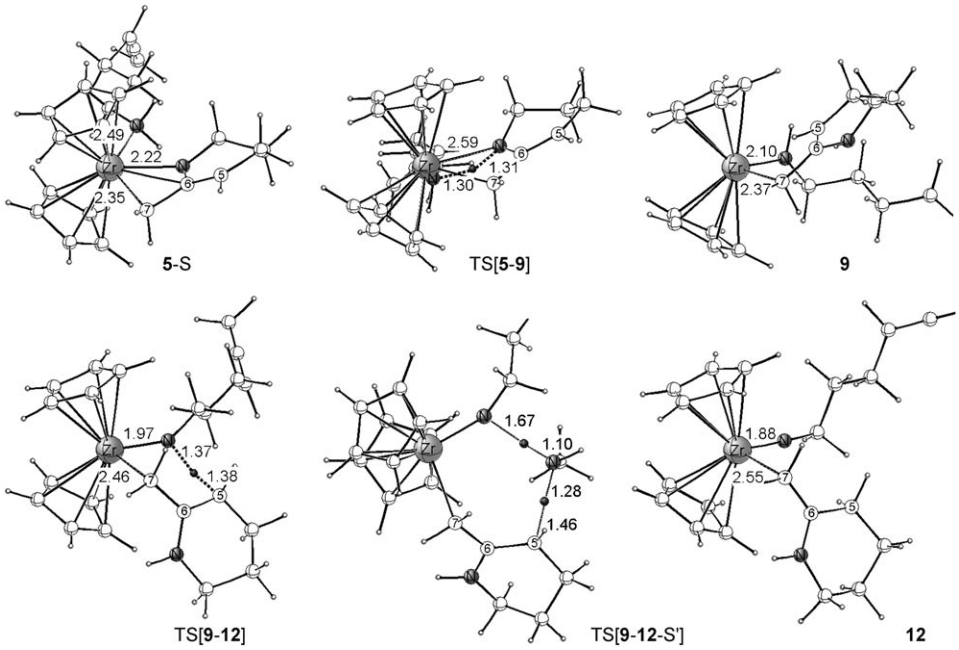

Figure 3. Selected structural parameters [Å] of the optimised structures of key species for protonolytic cleavage of the metallacycle in **5** by **1** to afford azacycle–amido–Zr compound **9** (top) and subsequent proton transfer to form cycloamine–imido–Zr complex **12** (bottom). See also Figures S8 and S9 in the Supporting Information. The cutoff for drawing Zr–C bonds was arbitrarily set to 2.8 Å. Please note that the amido-/imidoallene moiety is displayed in a truncated fashion for several of the species.

Catalytic reaction course for the IHC of aminoallenes

Gibbs free-energy profile: The condensed Gibbs free-energy profile, comprising solely of viable pathways for all relevant steps of the catalytic cycle (Schemes 2 and 5) is displayed in Scheme 6, in which **3′** was chosen as the reference species. The sequence of steps for the conversion of **2** into bis(amido)–Zr and imidoallene–Zr complexes is not included (see Scheme 4). The free-energy profile together with the exploration of individual elementary steps reported in previous sections leads to the following conclusions:

1) Substrate-free imidoallene–Zr species **3′**, which contains a chelating imidoallene functionality, is the catalyti-

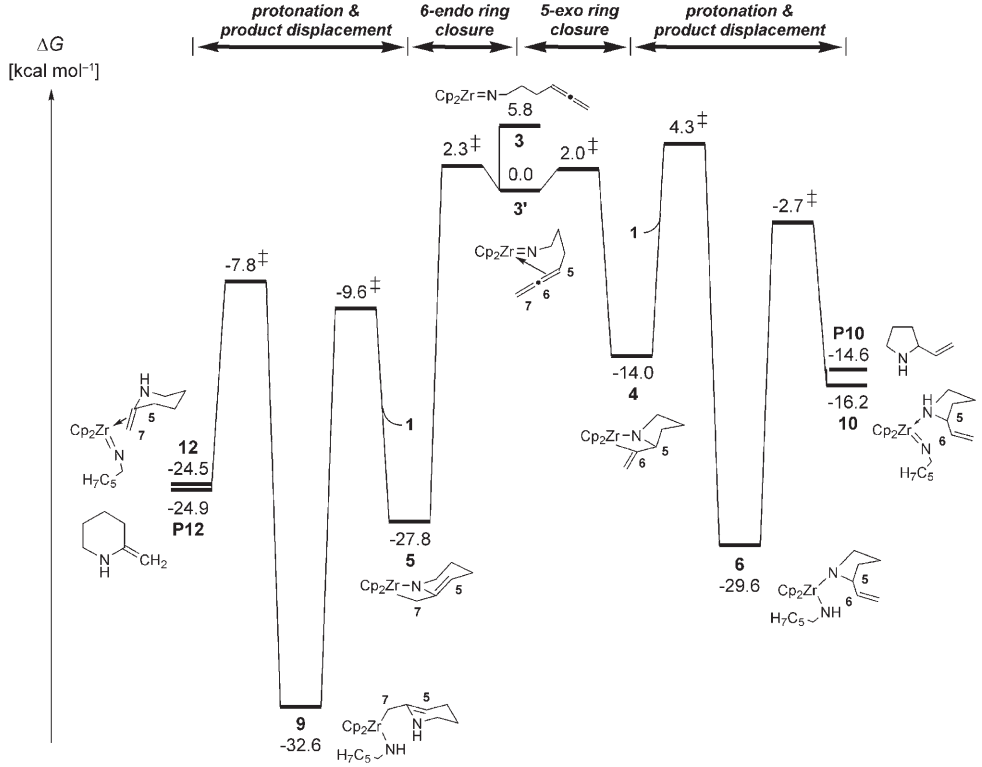

Scheme 6. Condensed Gibbs free-energy profile [kcal mol^{-1}] of the intramolecular hydroamination/cyclisation of **1** mediated by precatalyst **2**. Species **3′** is chosen as the reference and the sequence of steps for conversion of **2** into bis(amido)–Zr and imidoallene–Zr complexes is not included, see Scheme 4. Only the most feasible pathways for individual steps are included, whereas alternative, but unfavourable pathways are omitted for the sake of clarity. Cycloamine displacement through the **10**/**12**→**3′**+**P10**/**P12** pathway has been included.

cally active species that represents the direct precursor for the [2+2] cycloaddition reaction of the allenic C=C linkage across the Zr=N bond.

2) Ring closure is predicted to be a highly facile process. Almost identical free-energy barriers of only 2.0–2.3 kcal mol^{-1} are associated with the regioisomeric 5-*exo* and 6-*endo* pathways that yield **4** and **5**, respectively, in an exergonic process. The latter pathway is somewhat preferred thermodynamically.
3) The stepwise protonation of azazirconacyclobutane intermediates is predicted to be substantially slower than cycloaddition. Protonation takes place through a TS structure that constitutes the simultaneous cleavage of N–H bonds at the amido-/imidoallene moiety and formation of C–H or N–H bonds. The present study predicts that the protonation of **4** at carbon atom C^6 and subsequent α-hydrogen elimination through the **4**+**1**→**6**→**10**→**P10**+**3′** pathway is the most accessible route for the generation of five-membered allylamines. On the other hand, the six-membered cycloamine **P11′** is predominantly formed through the **5**+**1**→**9**→**12**→**3′**+**P12**⇄**P11′** pathway, firstly, by protonolyis of the Zr–N bond in **5** and subsequent proton transfer onto the carbon atom C^5 in **9**. Conceivable alternative pathways have been shown to be energetically disfavoured.
4) Of the two consecutive proton transfer steps, the second one determines the overall kinetics of the entire protonation process. Additional substrate appears to accelerate the second proton transfer along the favourable **4**→**P10** and **5**→**P12** pathways, which have free-energy barriers of 26.9 and 24.8 kcal mol^{-1}, respectively.
5) As revealed from Scheme 4, the **1**+**2**→**I1**(+CH_4)→**3′**-(+2CH_4)+(**1**)⇄**3**-S⇄**BA** sequence of steps is the favourable route for the conversion of precatalyst **2** into the bis(amido)–Zr complex. Compound **BA** is likely to be the thermodynamically prevalent, but dormant, species within the catalytic reaction course. The reversible α-elimination of **1** from **BA**[16a,26] to form active species **3′** is associated with a free-energy barrier of 31.3 kcal mol^{-1} and is uphill ($\Delta G = 21.1$ kcal mol^{-1}).
6) Accordingly, this process is rate determining, in which **3′** is a transient species that becomes immediately transformed into **4** and **5**. This scenario is similar to the mechanism established for intermolecular hydroamination of alkynes and allenes mediated by using bis(amido)–Zr complexes.[16a]

Factors governing the product composition: As revealed from the computational exploration reported thus far, ring closure and protonolysis are the steps that control the reaction outcome. Intramolecular addition of the allenic C=C linkage across the Zr=N bond is the step that dictates whether five- or six-membered azacycles are formed. This process is kinetically highly facile and strongly exergonic, and almost identical kinetics ($\Delta\Delta G^{\neq} = 0.3$ kcal mol^{-1}) is predicted for the two regioisomeric pathways. Thus, ring closure does not proceed regioselectively and both azazirconacyclobutane intermediates **4** and **5** are likely to be formed in comparable amounts.[34]

Subsequent stepwise proton transfer is clearly significantly slower. The protonation of **4** and **5** following the most feasible **4**+**1**→**6**→**10**→**3′**+**P10** and **5**+**1**→**9**→**12**→**3′**+**P12**⇄**P11′** routes has overall free-energy barriers of 26.9 and 24.8 kcal mol^{-1}, respectively. Hence, **5** is predicted to display a larger propensity for protonolytic cleavage than **4**. The calculated kinetic gap ($\Delta\Delta G^{\neq} = 2.1$ kcal mol^{-1})[35] reveals that both routes are accessible, and hence, **P10** and **P11′** are among the reaction products, **P11′** being the prevalent cycloamine. As both the TS structures for proton transfer and also the azacycle-amido–Zr compounds are sensitive to steric constraints, the delicate balance between the cycloamine-generating routes is likely to change upon the introduction of steric demands. Thus, substrates that are sterically more encumbered than **1** can act to distinguish between alternative protonation pathways, thereby regulating the composition of five- and six-membered cycloamines.

Conclusion

Presented herein is what is believed to be the first comprehensive computational exploration of the salient mechanistic features of the IHC of aminoallenes promoted by a neutral zirconocene catalyst. It encompasses the complete catalytic cycle (Scheme 2) for cyclohydroamination of **1** by precatalyst **2**. The mechanistic conclusions drawn herein are based on the Gibbs free-energy profile of the entire reaction that has been obtained by employing a reliable DFT method. The present study complements the mechanistic insights revealed from experiments by a detailed computational characterisation of structural and energetic aspects of alternative pathways for all relevant elementary steps.

The operative mechanism entails the initial transformation of precatalyst **2** into a bis(amido)–Zr compound in the presence of substrate **1**. This complex is likely to be the thermodynamically prevalent, but dormant, species within the catalytic reaction course. It undergoes a reversible, rate-determining α-elimination of **1** to form imidoallene–Zr compound **3′** that has a chelating imidoallene functionality. This catalytically active species is rapidly transformed into azazirconacyclobutane intermediates through the addition of the allenic C=C linkage across the Zr=N bond. This is a highly facile process that does not occur in a regioselective fashion, because the alternative pathways for the formation of five- and six-membered azacycles show comparable probabilities. Degradation of the cyclobutane moiety through the most feasible pathways involves the initial protonolysis of the metallacycle moiety by the aminoallene substrate and subsequent proton transfer from the Zr–NHR moiety onto the azacycle. The five-membered allylamine is generated by protonation at carbon atom C^6 and subsequent α-hydrogen elimination, whereas protonolysis of the cyclobutane moiety at the Zr–N bond followed by proton transfer onto carbon

atom C^5 is the dominant route for the formation of the six-membered product. Of the two consecutive proton-transfer steps, the second one determines the overall kinetics of the protonation process. Protonation is predicted to be significantly slower than ring closure. The factors that regulate the composition of cycloamine products have been elucidated.

[1] For reviews of catalytic hydroamination, see: a) L. S. Hegedus, *Angew. Chem.* **1988**, *100*, 1147; *Angew. Chem. Int. Ed.* **1998**, *27*, 1113; b) D. M. Roundhill, *Catal. Today* **1997**, *37*, 155; c) T. E. Müller, M. Beller, *Chem. Rev.* **1998**, *98*, 675; d) M. Nobis, B. Driessen-Hölscher, *Angew. Chem.* **2001**, *113*, 4105; *Angew. Chem. Int. Ed.* **2001**, *40*, 3983; e) R. Taube in *Applied Homogeneous Catalysis with Organometallic Complexes* (Eds.: B. Cornils, W. A. Herrmann), Wiley-VCH, Weinheim, **2002**, pp. 513–524; f) J. Seayad, A. Tillack, C. G. Hartung, M. Beller, *Adv. Synth. Catal.* **2002**, *344*, 795; g) F. Pohlki, S. Doye, *Chem. Soc. Rev.* **2003**, *32*, 104; h) P. W. Roesky, T. E. Müller, *Angew. Chem.* **2003**, *115*, 2812; *Angew. Chem. Int. Ed.* **2003**, *42*, 2708; i) J. F. Hartwig, *Pure Appl. Chem.* **2004**, *76*, 507; j) K. C. Hultzsch, *Adv. Synth. Catal.* **2005**, *347*, 367.

[2] For cyclohydroamination mediated by rare-earth metals, see: a) Y. K. Kim, T. Livinghouse, *Angew. Chem.* **2002**, *114*, 3797; *Angew. Chem. Int. Ed.* **2002**, *41*, 3645; b) Y. K. Kim, T. Livinghouse, Y. Horino, *J. Am. Chem. Soc.* **2003**, *125*, 9560; c) P. N. O'Shaughnessy, P. D. Knight, C. Morton, K. M. Gillespie, P. Scott, *Chem. Commun.* **2003**, *14*, 1770; d) D. V. Gribkov, K. C. Hultzsch, F. Hampel, *Chem. Eur. J.* **2003**, *9*, 4796; e) S. Hong, A. M. Kawaoka, T. J. Marks, *J. Am. Chem. Soc.* **2003**, *125*, 15878; f) J. Collin, J.-C. Duran, E. Schulz, A. Trifonov, *Chem. Commun.* **2003**, 3048; g) F. Lauterwasser, P. G. Hayes, St. Bräse, W. E. Piers, L. L. Schafer, *Organometallics* **2004**, *23*, 2234; h) D. V. Gribkov, K. C. Hultzsch, *Chem. Commun.* **2004**, 730; i) K. C. Hultzsch, F. Hampel, Th. Wagner, *Organometallics* **2004**, *23*, 2601; j) J. Y. Kim, T. Livinghouse, *Org. Lett.* **2005**, *7*, 4391.

[3] For cyclohydroamination mediated by Group 4 transition metals, see: a) P. L. McGrane, T. Livinghouse, *J. Org. Chem.* **1992**, *57*, 1323; b) P. L. McGrane, M. Jensen, T. Livinghouse, *J. Am. Chem. Soc.* **1992**, *114*, 5459; c) P. L. McGrane, T. Livinghouse, *J. Am. Chem. Soc.* **1993**, *115*, 11485; d) I. Bytschkov, S. Doye, *Tetrahedron Lett.* **2002**, *43*, 3715; e) C. Li, R. K. Thomson, B. Gillon, B. O. Patrick, L. L. Schafer, *Chem. Commun.* **2003**, 2462; f) D. V. Gribkov, K. C. Hultzsch, *Angew. Chem.* **2004**, *116*, 5659; *Angew. Chem. Int. Ed.* **2004**, *43*, 5542; g) P. A. Knight, I. Munslow, P. N. O'Shaughnessy, P. Scott, *Chem. Commun.* **2004**, 894; h) J. A. Bexrud, J. D. Beard, D. C. Leitch, L. L. Schafer, *Org. Lett.* **2005**, *7*, 1959; i) H. Kim, P. H. Lee, T. Livinghouse, *Chem. Commun.* **2005**, 5205.

[4] For cyclohydroamination mediated by late-transition metals, see: a) T. E. Müller, M. Grosche, E. Herdtweck, A.-K. Pleier, E. Walter, Y.-K. Yan *Organometallics* **2000**, *19*, 170; b) T. Kondo, T. Okada, T. Suzuki, T. Mitsudo, *J. Organomet. Chem.* **2001**, *622*, 149; c) S. Burling, L. D. Field, B. A. Messerle, P. Turner, *Organometallics* **2004**, *23*, 1714; d) L. M. Lutete, I. Kadota, Y. Yamamoto, *J. Am. Chem. Soc.* **2004**, *126*, 1622; e) L. D. Field, B. A. Messerle, K. Q. Vuong, P. Turner, *Organometallics* **2005**, *24*, 4241; f) G. B. Bajracharya, Z. Huo, Y. Yamamoto, *J. Org. Chem.* **2005**, *70*, 4883; g) C. F. Bender, R. A. Widenhoefer, *J. Am. Chem. Soc.* **2005**, *127*, 1070; h) F. E. Michael, B. M. Cochran, *J. Am. Chem. Soc.* **2006**, *128*, 4246; i) A. Takemiya, J. F. Hartwig, *J. Am. Chem. Soc.* **2006**, *128*, 6042.

[5] For cyclohydroamination mediated by organolanthanides, see: a) M. R. Gagné, T. J. Marks, *J. Am. Chem. Soc.* **1989**, *111*, 4108; b) M. R. Gagné, T. J. Marks, *J. Am. Chem. Soc.* **1992**, *114*, 275; c) Y. Li, P.-F. Fu, T. J. Marks, *Organometallics* **1994**, *13*, 439; d) Y. Li, T. J. Marks, *J. Am. Chem. Soc.* **1996**, *118*, 9295; e) G. A. Molander, E. D. Dowdy, *J. Org. Chem.* **1998**, *63*, 8983; f) M. R. Bürgstein, H. Berberich, P. W. Roesky, *Organometallics* **1998**, *17*, 1452; g) A. T. Gilbert, B. L. Davis, T. J. Emge, R. D. Broene, *Organometallics* **1999**, *18*, 2125; h) G. A. Molander, E. D. Dowdy, *J. Org. Chem.* **1999**, *64*, 6515; i) Y. K. Kim, T. Livinghouse, J. E. Bercaw, *Tetrahedron Lett.* **2001**, *42*, 2944; j) G. A. Molander, E. D. Dowdy, S. K. Pack, *J. Org. Chem.* **2001**, *66*, 4344; k) M. R. Bürgstein, H. Berberich, P. W. Roesky, *Chem. Eur. J.* **2001**, *7*, 7078; l) S. Hong, T. J. Marks, *J. Am. Chem. Soc.* **2002**, *124*, 7886; m) S. Hong, S. Tian, M. V. Metz, T. J. Marks, *J. Am. Chem. Soc.* **2003**, *125*, 14768; n) A. Zulys, T. K. Panda, M. T. Gamer, P. W. Roesky, *Chem. Commun.* **2004**, 2584.

[6] a) G. A. Molander, J. A. C. Romero, *Chem. Rev.* **2002**, *102*, 2161; b) S. Hong, T. J. Marks, *Acc. Chem. Res.* **2004**, *37*, 673.

[7] a) M. R. Crimmin, I. J. Caseley, M. S. Hill, *J. Am. Chem. Soc.* **2005**, *127*, 2042; b) X. Han, R. A. Widenhoefer, *Angew. Chem.* **2006**, *118*, 1779; *Angew. Chem. Int. Ed.* **2006**, *45*, 1744.

[8] a) A. Zulys, M. Dochnahl, D. Hollmann, K. Löhnwitz, J.-S. Herrmann, P. W. Roesky, S. Blechert, *Angew. Chem.* **2005**, *117*, 7972; *Angew. Chem. Int. Ed.* **2005**, *44*, 7794; b) M. Dochnahl, J.-W. Pissarek, S. Blechert, K. Löhnwitz, P. W. Roesky, *Chem. Commun.* **2006**, 3405.

[9] a) I. Bytschkov, S. Doye, *Eur. J. Org. Chem.* **2003**, 935; b) A. L. Odom, *Dalton Trans.* **2005**, 225.

[10] a) T. J. Marks, R. D. Ernst in *Comprehensive Organometallic Chemistry* (Eds.: G. Wilkinson, F. G. A. Stone, E. W. Abel), Pergamon, Oxford, **1982**, Chapter 21; b) W. J. Evans, *Adv. Organomet. Chem.* **1985**, *24*, 131; c) C. J. Schaverien, *Adv. Organomet. Chem.* **1994**, *36*, 283; d) H. Schumann, J. A. Meese-Marktscheffel, L. Esser, *Chem. Rev.* **1995**, *95*, 865; e) F. T. Edelmann in *Comprehensive Organometallic Chemistry* (Eds.: G. Wilkinson, F. G. A. Stone, E. W. Abel), Pergamon, Oxford, **1995**, Chapter 2; f) R. Anwander, W. A. Herrmann, *Top. Curr. Chem.* **1996**, *179*, 1; g) F. T. Edelmann, *Top. Curr. Chem.* **1996**, *179*, 247; h) *Topics in Organometallic Chemistry, Vol. 2* (Ed.: S. Kobayashi), Springer, Berlin, **1999**; i) M. N. Bochkarev, *Chem. Rev.* **2002**, *102*, 2089; j) S. Arndt, J. Okuda, *Chem. Rev.* **2002**, *102*, 1953; k) F. T. Edelmann, D. M. M. Freckmann, H. Schumann, *Chem. Rev.* **2002**, *102*, 1851; l) H. C. Aspinall, *Chem. Rev.* **2002**, *102*, 1807.

[11] For cyclohydroamination of aminoallenes by titanium tetrakisamido, zirconium bis(sulfonamido) and zirconocene compounds, see: a) L. Ackermann, R. G. Bergman, *Org. Lett.* **2002**, *4*, 1475; b) L. Ackermann, R. G. Bergman, R. N. Loy, *J. Am. Chem. Soc.* **2003**, *125*, 11956.

[12] For cyclohydroamination of aminoallenes by titanium amino-alcohol compounds, see: a) J. M. Hoover, J. R. Petersen, J. M. Pikul, A. R. Johnson, *Organometallics* **2004**, *23*, 4614; b) J. R. Petersen, J. M. Hoover, W. S. Kassel, A. L. Rheingold, A. R. Johnson, *Inorg. Chim. Acta* **2005**, *358*, 687.

[13] a) M. R. Gagné, C. L. Stern, T. J. Marks, *J. Am. Chem. Soc.* **1992**, *114*, 275; b) V. M. Arredondo, F. E. McDonald, T. J. Marks, *J. Am. Chem. Soc.* **1998**, *120*, 4871.

[14] For computational studies of organolanthanide-assisted intramolecular hydroamination/cyclisation of various substrate classes, see: a) A. Motta, G. Lanza, I. L. Fragala, T. J. Marks, *Organometallics* **2004**, *23*, 4097; b) S. Tobisch, *J. Am. Chem. Soc.* **2005**, *127*, 11979; c) S. Tobisch, *Chem. Eur. J.* **2006**, *12*, 2520.

[15] For a computational study of the cationic Group 4 metal-assisted intramolecular hydroamination/cyclisation of aminoallenes, see: S. Tobisch, *Dalton Trans.* **2006**, 4277.

[16] a) P. J. Walsh, A. M. Baranger, R. G. Bergman, *J. Am. Chem. Soc.* **1992**, *114*, 1708; b) A. M. Baranger, P. J. Walsh, R. G. Bergman, *J. Am. Chem. Soc.* **1993**, *115*, 2753; c) S. Y. Lee, R. G. Bergman, *Tetrahedron* **1995**, *51*, 4255; d) J. S. Johnson, R. G. Bergman, *J. Am. Chem. Soc.* **2001**, *123*, 2923.

[17] a) F. Pohlki, S. Doye, *Angew. Chem.* **2001**, *113*, 2361; *Angew. Chem. Int. Ed.* **2001**, *40*, 2305; b) Y. Li, Y. Shi, A. L. Odom, *J. Am. Chem. Soc.* **2004**, *126*, 1794; c) B. D. Ward, A. Maisse-Francois, P. Mountford, L. H. Gade, *Chem. Commun.* **2004**, 704.

[18] For a computational study of the neutral Group 4 metal-assisted intermolecular hydroamination, see: B. F. Straub, R. G. Bergman, *Angew. Chem.* **2001**, *113*, 4768; *Angew. Chem. Int. Ed.* **2001**, *40*, 4632.

[19] a) V. M. Arredondo, F. E. McDonald, T. J. Marks, *J. Am. Chem. Soc.* **1998**, *120*, 4871; b) V. M. Arredondo, S. Tian, F. E. McDonald, T. J.

Marks, *J. Am. Chem. Soc.* **1999**, *121*, 3633; c) V. M. Arredondo, F. E. McDonald, T. J. Marks, *Organometallics* **1999**, *18*, 1949.
[20] a) S. Arseniyadis, J. Gore, *Tetrahedron Lett.* **1983**, *24*, 3997; b) R. Kinsman, D. Lathbury, P. Vernon, T. Gallagher, *J. Chem. Soc. Chem. Commun.* **1987**, 243; c) D. N. A. Fox, T. Gallagher, *Tetrahedron* **1990**, *46*, 4697; d) M. Al-Masum, M. Meguro, Y. Yamamoto, *Tetrahedron Lett.* **1997**, *38*, 6071; e) M. Meguro, Y. Yamamoto, *Tetrahedron Lett.* **1998**, *39*, 5421.
[21] a) R. Ahlrichs, M. Bär, M. Häser, H. Horn, C. Kölmel, *Chem. Phys. Lett.* **198**9, 162, 165; b) O. Treutler, R. Ahlrichs, *J. Chem. Phys.* **199**5, 102, 346; c) K. Eichkorn, O. Treutler, H. Öhm, M. Häser, R. Ahlrichs, *Chem. Phys. Lett.* **1995**, *242*, 652.
[22] a) P. A. M. Dirac, *Proc. Cambridge Philos. Soc.* **193**0, 26, 376; b) J. C. Slater, *Phys. Rev.* **1951**, *81*, 385; c) S. H. Vosko, L. Wilk, M. Nussair, *Can. J. Phys.* **1980**, *58*, 1200; d) A. D. Becke, *Phys. Rev.* **1988**, *A38*, 3098; e) J. P. Perdew, *Phys. Rev.* **1986**, *B33*, 8822; *Phys. Rev.* **1986**, *B34*, 7406.
[23] a) A. Klamt, G. Schüürmann, *J. Chem. Soc. Perkin Trans. 2* 1993, 799; b) A. Klamt in *Encyclopedia of Computational Chemistry, Vol. 1* (Ed.: P. von R. Schleyer), Wiley, Chichester, **1998**, pp. 604–615.
[24] For further details, see: http://www.struked.de.
[25] Examination by a linear-transit approach gave no indication that this process is associated with a significant enthalpic barrier.
[26] P. J. Walsh, F. J. Hollander, R. G. Bergman, *Organometallics* **1993**, *12*, 3705.
[27] For the **I1**$+$**1**$\rightarrow$**BA**$+CH_4$ conversion (pathway B, Scheme 3), a rate of $\approx 5\times10^{-5}\,s^{-1}$ (358.15 K) has been reported for the methyl–amido–Zr complex $[ZrCp_2(Me)(NH\text{-}4\text{-}CMe_3C_6H_4)]$ in the presence of 4-*tert*-butylaniline (see ref. [26]). This rate corresponds to a value of about 28.1 kcal mol^{-1} for $\Delta G^{\neq}$ for the step that has the highest barrier (**I1**$\rightarrow$**3′**$+CH_4$, Scheme 2), by application of the Eyring equation with $k=(2.08\times10^{10})\times T\times\exp(-\Delta G^{\neq}/RT)$.
[28] Please bear in mind that steric congestion introduced by employing bulky substrates is known to greatly affect the relative stability of the **3**, **3′**, **3**-S, **3d** and **BA** species and also the kinetics for α-elimination (see, for instance, ref. [17a,18]).
[29] Bis(amido)–Zr compound **BA** and the dimer **3d** are both dormant species.
[30] a) H. M. Senn, P. E. Blöchl, A. Togni, *J. Am. Chem. Soc.* **2000**, *122*, 4098; b) S. Ilieva, B. Galabov, D. G. Musaev, K. Morokuma, H. F. Schaefer, III, *J. Org. Chem.* **2003**, *68*, 1496.
[31] The rotational isomerisation of the azacycle moiety in **9** (rotation around the $Zr-C^7$ bond, see Scheme 5) is a facile process that is associated with a small barrier of $\approx$5.3 kcal mol^{-1}. See Figure S10 in the Supporting Information for more details. Rotation of the azacycle moiety in **8** (rotation around the $N-C^6$ bond, see Scheme 5) along the **8**$\rightarrow$**11′** pathway occurs simultaneously with proton transfer.
[32] Cycloamine product release through the **12**$\rightarrow$**P12**$+$**3′** pathway is kinetically facile (ref. [25]) and is almost thermoneutral ($\Delta G=-0.4$ kcal mol^{-1}).
[33] The 1,3-hydrogen shift is presumably a viable process. The kinetics of this process has not been investigated in the present study.
[34] Despite the larger enthalpy for **3′**$\rightarrow$**5**, intermediates **4** and **5** should be formed in comparable amounts because the catalytic process does not occur under thermodynamic control.
[35] The calculated $\Delta\Delta G^{\neq}$ gap of 2.1 kcal mol^{-1} corresponds to a **P11′**/**P10** ratio of 97:3 (298.15 K) on application of Maxwell–Boltzmann statistics. It is in reasonable agreement with the observed product composition of 16:3, which transforms into $\Delta\Delta G^{\neq}=1.0$ kcal mol^{-1} (298.15 K).

Received: September 7, 2006
Published online: March 13, 2007

